The Evaluation of a Low Powered Microwave Induced Plasma as an Atom Cell for Atomic Spectrometry

by

Larry D. Perkins

Thesis submitted to the Faculty of the
Virginia Polytechnic Institute and State University
in partial fulfillment of the requirements for the degree of

MASTER OF SCIENCE

in

Analytical Chemistry

APPROVED:

Gary L. Long, Chairman

H. M. McNair

L. T. Taylor

The Evaluation of a Low Powered Microwave Induced Plasma as an Atom Cell for Atomic Spectrometry

by

Larry D. Perkins

Committee Chairman: Gary L. Long
Chemistry

(ABSTRACT)

The range of plasma spectroscopy tends to increase with the introduction of more efficient plasma excitation sources. In this thesis the use of one such plasma excitation source, the microwave induced plasma is evaluated as an atom cell for atomic spectrometry. The modes of spectrometry evaluated are atomic emission and atomic fluoresence.

Analytical merits of the microwave induced plasma using detection limits and studies of interelement effects (i.e. vaporization, ionization, and scatter interferences) are also presented.

ACKNOWLEDGEMENTS

To my mother, , thank you for your love, patience, and support during my stay at Virginia Tech.

Dr. Gary Long, thanks for believing in me. Your help and understanding has added to my lamp of knowledge the fuel of human understanding and a scientific sense. I hope that it will serve me well through the joys and challanges of my life. Thanks also goes to your family members: , , and .

To Dr. H. M. McNair, Dr. James Wolfe, and Dr. L. T. Taylor, thank you for scientific and personal help during my stay at Virginia Tech.

To my friend , thanks goes to you and your parents ( ) for giving me a home away from home.

To the members of my research group, the "Plasmen" ( ), thanks for conversations that have provided scientific stimulation. your expertise in editing has been insurmountable.

TABLE OF CONTENTS

LIST OF TABLES

LIST OF FIGURES

CHAPTER 1

LITERATURE REVIEW

Due to the sudden interest in trace chemical analysis, plasma excitation sources have become very popular. The most commonly used plasma excitation sources are the inductively coupled plasma (ICP), direct current plasma (DCP), and microwave induced plasma (MIP). The ICP and DCP are most commonly used for the qualitative and quantative determination of liquids, solids, and gases. Unlike the ICP and DCP, the MIP has been most frequently used as a selective detector for gas chromatography due to its inability to efficiently excite liquid samples.

The microwave induced plasma, MIP, is essentially a plasma discharge of helium, argon, nitrogen, or air. The MIP is maintained by a plasma supporting structure (resonance cavity, etc.) which is a hollow metal container which allows a standing electromagnetic wave to be established within it, or along it. Since the standing wave is at microwave frequencies (usually 2450 MHz) its size is on the order of 9-10 centimeters [1].

To generate the standing wave, microwave energy is sent into the cavity by means of a circuit loop, circuit short, or antenna which is in turn connected to a microwave power supply via a coaxial cable or waveguide. The plasma gas is then passed through the cavity, is ionized, and energy is

coupled to the gaseous ions to produce the discharge. Various transverse electric and magnetic waves enable such a configuration to exist.

In this thesis, a different view of the use of the microwave induced plasma as an analytical tool for trace elemental analysis will be presented. In chapter 2, atomic emission is used as a diagnostic tool to conduct comparative studies between proposed atomic fluoresence detection and present plasma atomic emission. Chapter 3 presents atomic fluoresence as an alternative to atomic emission with the microwave plasma. Detection limits as well as interelement effects are presented using atomic emission spectrometry and atomic fluoresence spectrometry.

Cavity Nomenclature

Microwave cavities are differentiated by the pattern of their internal electro-magnetic field as either transverse electric, TE_{mnp}, modes or as transverse-magnetic, TM_{mnp}, modes [2]. In the TE_{mnp} mode the electric field E has no z component, while in the TM_{mnp} mode the magnetic field H has no z component. The subscripts m, n, p are intergers which further describe the internal magnetic field patterns by the number of repetitions in the E and H fields along their respective coordinate system (Figure 1-1). For a rectangular cavity with dimensions a, b, and L

aligned with the x, y, and z axis:

m = the number of half-period variations of E and H along x,

n = the number of half-period variations of E and H along y,

p = the number of half-period variations of E and H along z.

This principle also applies to a cylindrical cavity with coordinates θ, r, and z and with dimensions D and L the integers are defined as:

m = the number of half-period variations of E_r (for TE modes) or H_r (for TM modes) with respect to θ;

n = the number of half-period variations of E_θ (for TE modes) or H_θ (for TM modes) with respect to r;

p = the number of half-period variations of E_r (for TE modes) or H_r (for TM modes) with respect to z.

Cavity Materials

The efficiency of microwave cavities greatly depends on the physical characteristics of the metal used in construction. The ideal design must incorporate a metal of high conductivity and small skin depth. The skin depth is important since microwave radiation is known to penetrate some distance into the cavity walls. In order to minimize energy lost to the wall and maximize the quality factor,Q, of the cavity, the skin depth must be as small as possible [3]. The skin depths most commonly used in the construction of the resonant cavities at 2450 MHz are as follows:

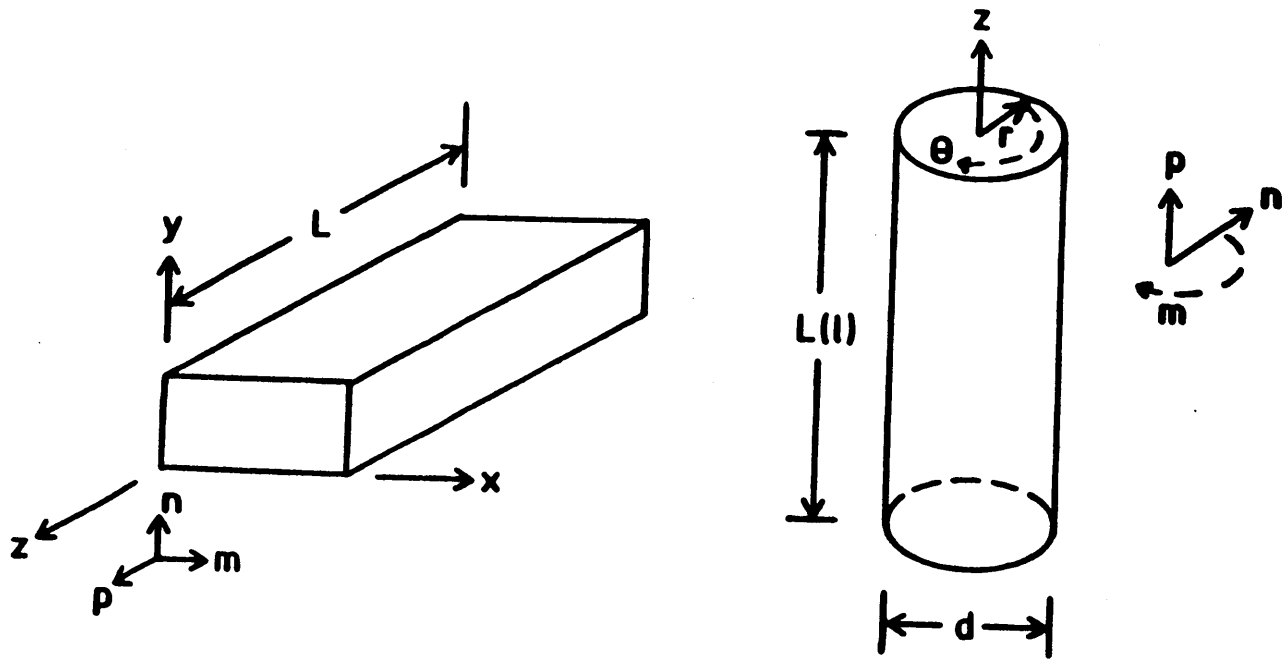

FIGURE 1-1: Coordination system used for microwave cavities.

silver	1.3 μm
copper	1.3 μm
gold	1.6 μm
aluminum	1.6 μm
brass	2.7 μm

The choice for the cavity depends upon a compromise of factors. For the highest Q, pure silver would be the best, with copper second and gold third. However, these pure metals are difficult to machine and the resulting cavity is marred, which reduces the Q. Futhermore, both pure copper and silver corrode rapidly in air and lose there high conductivity advantage. Because of this, the ideal cavity does not allow construction of the best cavities. Overall, aluminum stands to be the best choice for its low price and ease of machining. Another choice would be to machine a material of lower Q and coat the surface with a material of higher Q (i.e. Ag coated on brass, etc).

The Beenakker TM_{010} Cavity

The most frequently used microwave cavity today is the Beenakker cavity and is described below. Modifications of the original design are also presented. The modification by Boss and Riddle is discussed extensively since this type of cavity was used for completion of this thesis.

The cylindrical resonant cavity was first described by

Beenakker in 1976 [4]. In his design microwave energy is transfered to the cavity via a coupling loop connected to a coaxial connector at one end and grounded to the cavity face on the other end. The plane of the coupling was chosen to be perpendicular to the face of the cavity as illustrated in Figure 1-2.

The cavity operates in the transverse magnetic mode, TM. For a cavity operating in the TM_{010} mode, the values of m, n, and p must be zero, one, and zero respectively. In the TM_{010} mode, the resonance frequency depends upon the radial dimensions of the cavity. The proper diameter was calculated at 93.7 mm. This diameter is valid for a cavity operating in the absence of a plasma discharge. With the introduction of the plasma discharge and dielectrics (i.e. water and quartz) the resonance frequency will become lower. Therefore, the true diameter of the cavity must be smaller than the calculated value at 2450 MHz.

Previous cavities operated with helium at reduced pressures, the TM_{010} allowed operation of a stable helium plasma at atmospheric pressure.

Several modifications to the original Beenakker cavity allow improved operation. In one study van Dalen et.al.[5] published that ignition and tuning of the Beenakker design using metal screws is unreliable and yields excess heating

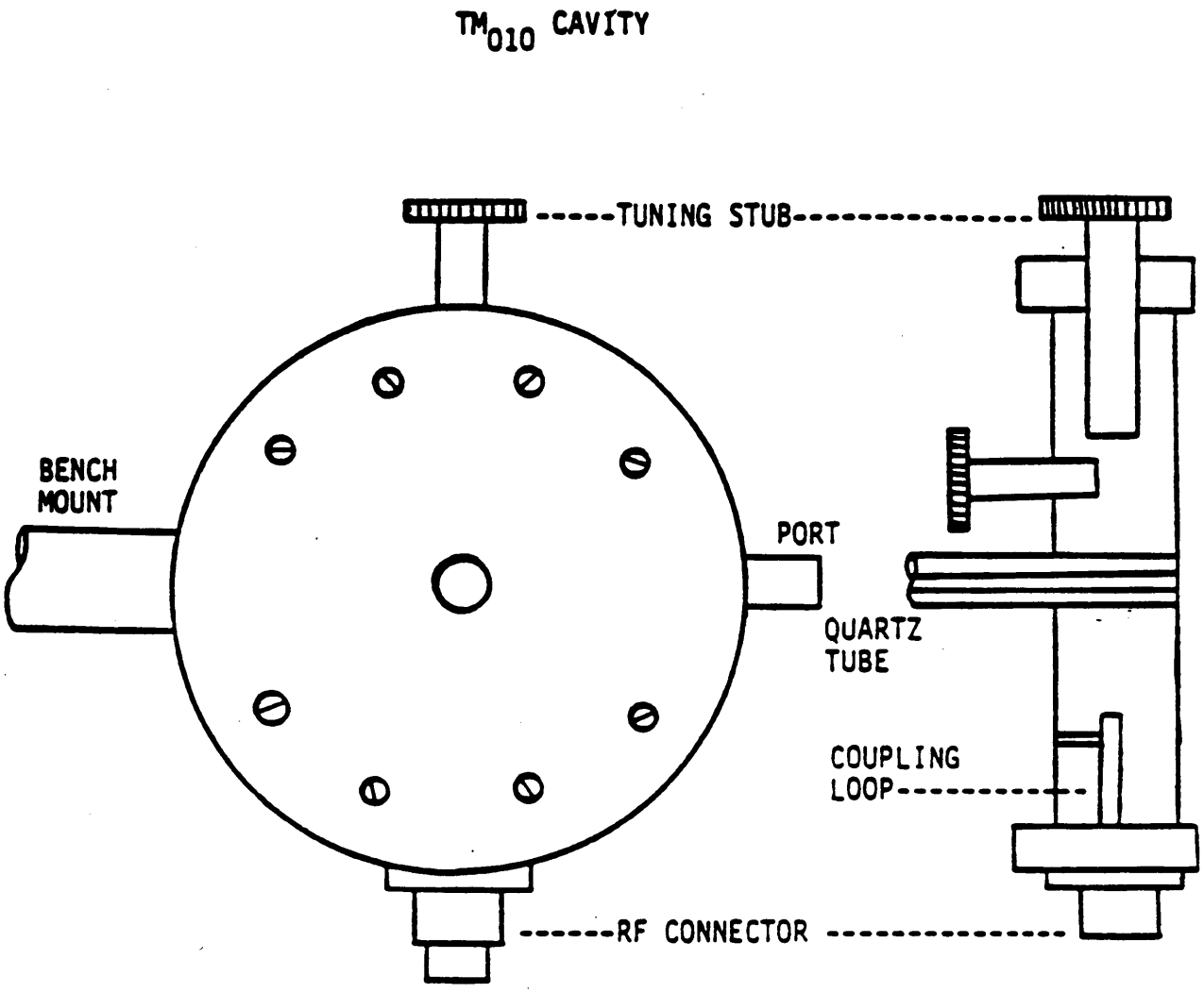

FIGURE 1-2: Schematic of the Beenakker cavity.

(power loss). van Dalen's modification substituted adjustable quartz rods for tuning screws and was able to have greater control over tuning and matching. The energy transfer was further improved by the addition of an Evenson 1/4-wave cavity to one face of the Beenakker cavity. Capacitive coupling was accomplished through the use of a variable length antenna rod, placed inside the center of the cavity, alongside and parallel to the cavity axis. This modification allowed for a larger tuning range and smaller cavity height.

In 1983 Boss and Riddle published their work on a highly efficient TM_{010} cavity [6] as shown in Fig. 1-3. This cavity is also a resonant cavity and was found to be 98% efficient from 10-100 W of applied power. The internal diameter of the cavity was fixed at 8.85 mm. A 7 mm diameter quartz rod, which provided tuning capabilities, extended into the cavity from a sidewall. Instead of employing a shorted tuning antenna for impedence matching, Boss and Riddle used a moveable antenna probe that could be translated across the face of cavity to achieve a 50 ohm impedance match between the generator and the load (cavity and/or plasma). The impedance, Z, is defined as the sum of the resistance, R, and the reactance, jX. The reactance is an imaginary term while resistance is a real term. In order to achieve a 50 ohm impedance between the generator and the

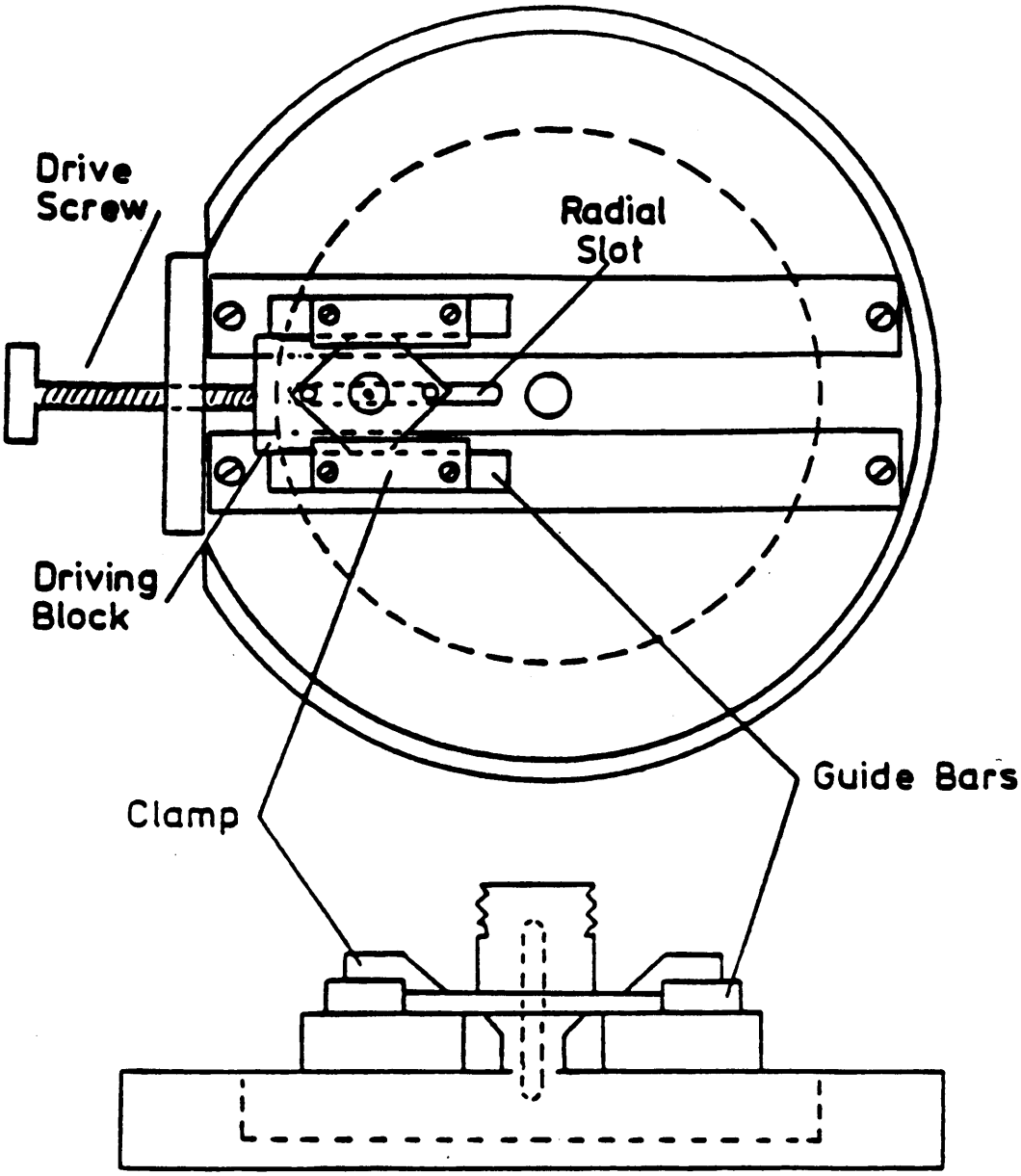

FIGURE 1-3: Schematic of the Highly Efficient TM_{010} cavity.

load, the generator impedance of 50 ohm has to be transformed into the load impedance by translating the coupling probe across the face of the cavity. As a result, the reactance term reduces to zero and the cavity and load operates with unit effiency (i.e. 50 ohms impedance matching). Thus the antenna probe was termed the "coupling probe" for the highly efficient cavity.

The coupling probes were fabricated from UG-58 A/U type N connectors. An extension of the center post was soldered a 10-gauge AW6 copper wire. The types of probes studied in the work were as follows: 1/4" ballbearing, a 10mm diameter disk, a hexagonal nut, a 12mm diameter disk, a 16mm diameter disk, a 3/8" ballbearing, and a 19mm diameter disk. Data produced showed, as the surface area of the probe increased so did the probe's ability to transfer power to the Ar plasma without increased reflected power. Using these coupling probes it was found that in the highly efficient cavity coupling is not purely capacitive or inductive at 2450 mHz.

Not only is the position of the probe along the face of the cavity important; the probe length or penetration depth into the cavity is equally important. Boss and Riddle found 92% penetration depth provided a better means of critically coupling the cavity since at shorter depths the probe does not allow sufficient coupling to the magnetic field in the

cavity.

Electric and magnetic field patterns of the cavity are shown in Figure 1-4 for both the loaded and unloaded case. The dotted lines represent the magnetic field while the solid line represents the electric field patterns in the cavity. For the unloaded case, the electric field is at a maximum at the center of the cavity while the magnetic field is at a maximum at the outer wall of the cavity. In the loaded case, the energy drawn by the plasma discharge only has a small change on the magnetic field. Therefore, for both cases the impedence increases as the probe is moved toward the center of the cavity.

Applied power into the cavity also plays a role in impedence matching. An increase in power lowers the cavity's impedence. As a result the position of the probe for a critically coupled cavity is dependent on the power introduced into the plasma.

A useful feature of the highly efficient cavity is that the cavity produces large plumes (4-16 cm); such an arrangement is particularly convenient when introducing aqueous samples into the plasma. Overall, Boss and Riddle modifications have created a more stable plasma that gives back the low power advantage to the microwave induced plasma.

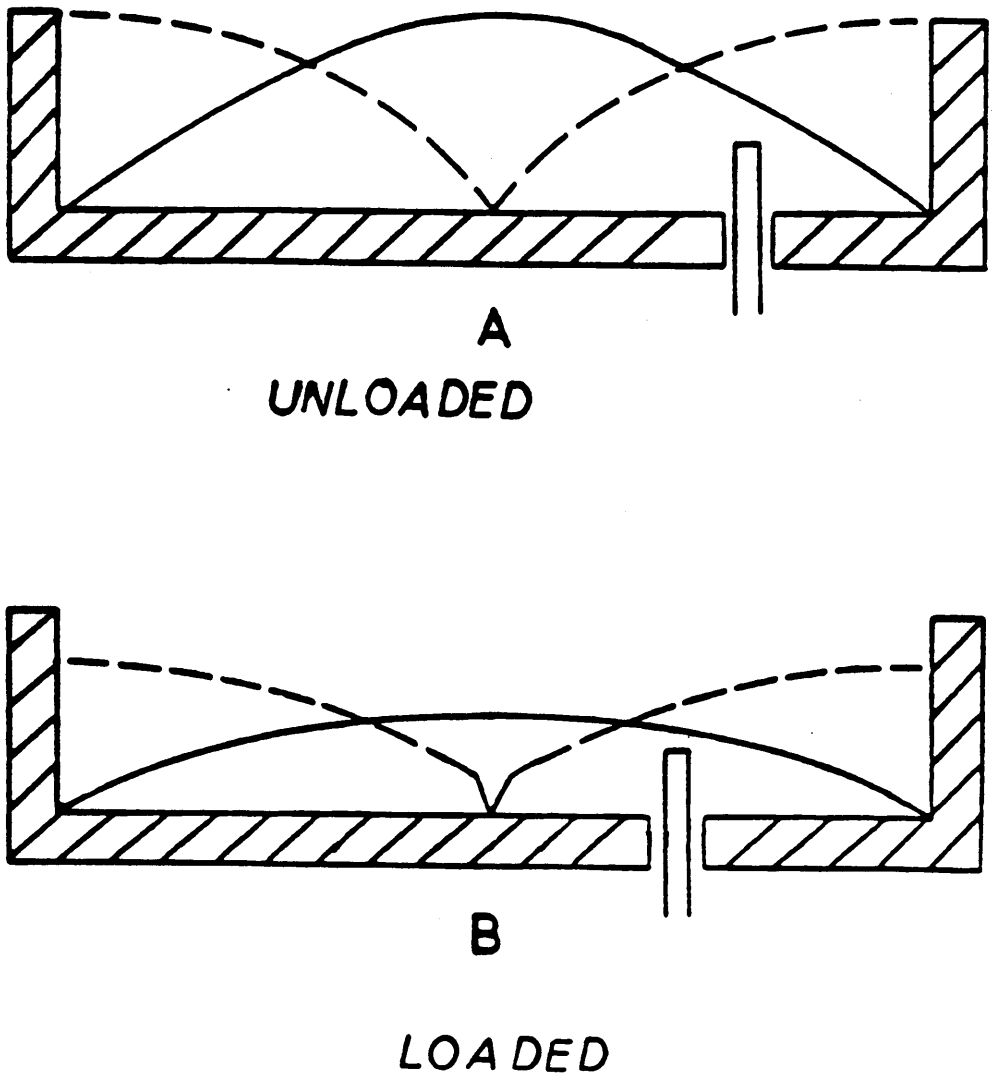

FIGURE 1-4: Electric and magnetic field patterns for the Highly Efficient TM_{010} cavity.

Sample Introduction

The microwave induced plasma in argon or helium possesses a number of advantages as an excitation source in atomic spectrometry. The MIP has a high excitation temperature of 4,000-6,000 K. This high excitation temperature allows for the excitation of halogens and nonmetals with relatively high sensitivity in the visible and ultraviolet regions.

A large variety of methods have been developed for sample introduction into the MIP; they include the following:

(1) introduction of gas chromatography eluents;

(2) sealed-cell introduction;

(3) nebulization of solutions;

(4) introduction by electrothermal vaporization;

(5) introduction via chemical formation of volatile substances.

These techniques have been discussed in recent reviews [1,7-10]. Only sample introduction via nebulization will be discussed here.

One of the most attractive aspect of liquid sample introduction is its relative simplicity and reliability; coupled with the fact that a sample dissolution step is often necessary to provide suitable statistics. This type of sample introduction has been called the Achilles Heel of

atomic spectrometry [11].

When liquid sample introduction systems are coupled to the MIP several problems arise. First, the MIP (compared to flames and plasmas) has a low kinetic temperature and low energy density which does not allow for sufficient vaporization and atomization. Second, the MIP is easily disturbed by the introduction of molecular vapors, such as those from the vaporized solvent. Water is particulary bad in this respect , having an absorption band at the operating frequency of the MIP, 2450 MHz.

Few papers have appeared on the subject of liquid sample introduction into the MIP. Beenakker et al [12] introduced aqueous samples into the plasma without desolvation at a sample uptake rate of 1.7 mL/min. A 150 W plasma was used to sustain the plasma. Satisfactory performance was obtained, but the use of the wet aerosol decreased the sensitivity by a factor of between 2 and 10, depending on the element studied.

Hass and Caruso was successful in introducing 0.81 mL/min of aqueous solution into a 500 W plasma for the study of metal ions in synthetic ocean water using a total Ar flow of 450 mL/min. Nebulizers included both concentric and frit types. Detection limits were comparable to the ICP. The authors reported severe microwave leakage using their 500 W argon plasma [13].

In a similar study, Ng and Shen [14] used a 105-115 W Ar plasma to introduce synthetic ocean water at a MAK nebulization uptake rate of 1.4 mL/min. The total Ar flow used in the study was reported at 537 mL/min. Detection limits compared favorably with the work of Beenakker.

CHAPTER 2

ATOMIC EMISSION SPECTROMETRY

A significant limitation to the use of the microwave induced plasma, MIP, for spectrochemical analysis is the problem of direct introduction of aqueous samples into the plasma. A MIP system employing a TM_{010} Beenakker cavity, Ar support gas, and applied power levels of less than 200 W does not possess sufficient plasma energy, density, and kinetic temperature to promote sufficient atomization and excitation of the analyte vapor [1]. During the past ten years, various investigators have tried different approaches to the problem of direct aqueous sample introduction.

One such approach focuses on the removal of water vapor from the analyte, so that the limited plasma energy is used in analyte vaporization and excitation instead of desolvation. This strategy involves the use of nebulizers and desolvation systems [8], electrothermal atomizers (heated wires and furnances) [15,16], and micro-arc atomizers [17].

Another approach to the problem of low energy density and plasma temperature utilizes higher applied power levels ranging from 300-800 W, sample introduction is usually achieved without the use of desolvation systems. However,

this method also results in severe cavity heating and significant microwave leakage due to inefficient power transfer to the cavity [13].

A third approach to this problem involves the mechanics of transfered power into the TM_{010} cavity. Hieftje calculates that, for the Beenakker cavity, only 35 W of applied microwave power is necessary to sustain a plasma with 1 L/min Ar and to support complete analyte desolvation and vaporization of a 1 mL/min aqueous sample [18]. This calculation is based on the assumption that the cavity is 100% efficient in power transfer. Unfortunately, the Beenakker cavity is much less than 100% efficient. Matus, Boss, and Riddle estimate that the Beenakker cavity uses only 25 W of forward power [6]. Power levels greater than that result in cavity and/or tuning stub heating. In an effort to increase the efficiency, Matus et al. modified the Beenakker cavity to increase the efficiency of power transfer [6]. This design, termed the highly efficient cavity, features an antenna probe that can be translated along the radial face of the cavity. This translation allows the probe to interact with the electric and magnetic fields to sense a 50 ohm load and thus provide a proper impedance match between the generator and the cavity. In a later study [19], the cavity was estimated to be 98% efficient in power transfer of applied power levels of

10-100 W.

In this chapter, studies on the use of this highly efficient TM_{010} cavity for the direct introduction of aqueous samples from a concentric nebulizer with no desolvation system and an applied power of only 70 W was employed. Using a tangential flow torch, we produced and sustained a torodial plasma with the output of the nebulizer alone. For charcterization of this low powered plasma, the limits of detection using atomic emission of refractory and non-refractory elements are presented, along with working curves and plasma profiles of elements of interest. Additionally, studies of ionization and vaporization interferences are described.

Experimental Setup

A block diagram of the experimental apparatus is shown in Figure 2-1; major components and manufactures of those components for the experimental setup are listed in Table 2-1. The optimized operational atomic emission parameters are listed in Table 2-2.

Operational Conditions

For plasma operation, a flow of 1 L/min of argon gas was introduced through the side inlet of the plasma torch with a pressure of 50 PSI of argon gas from the nebulizer.

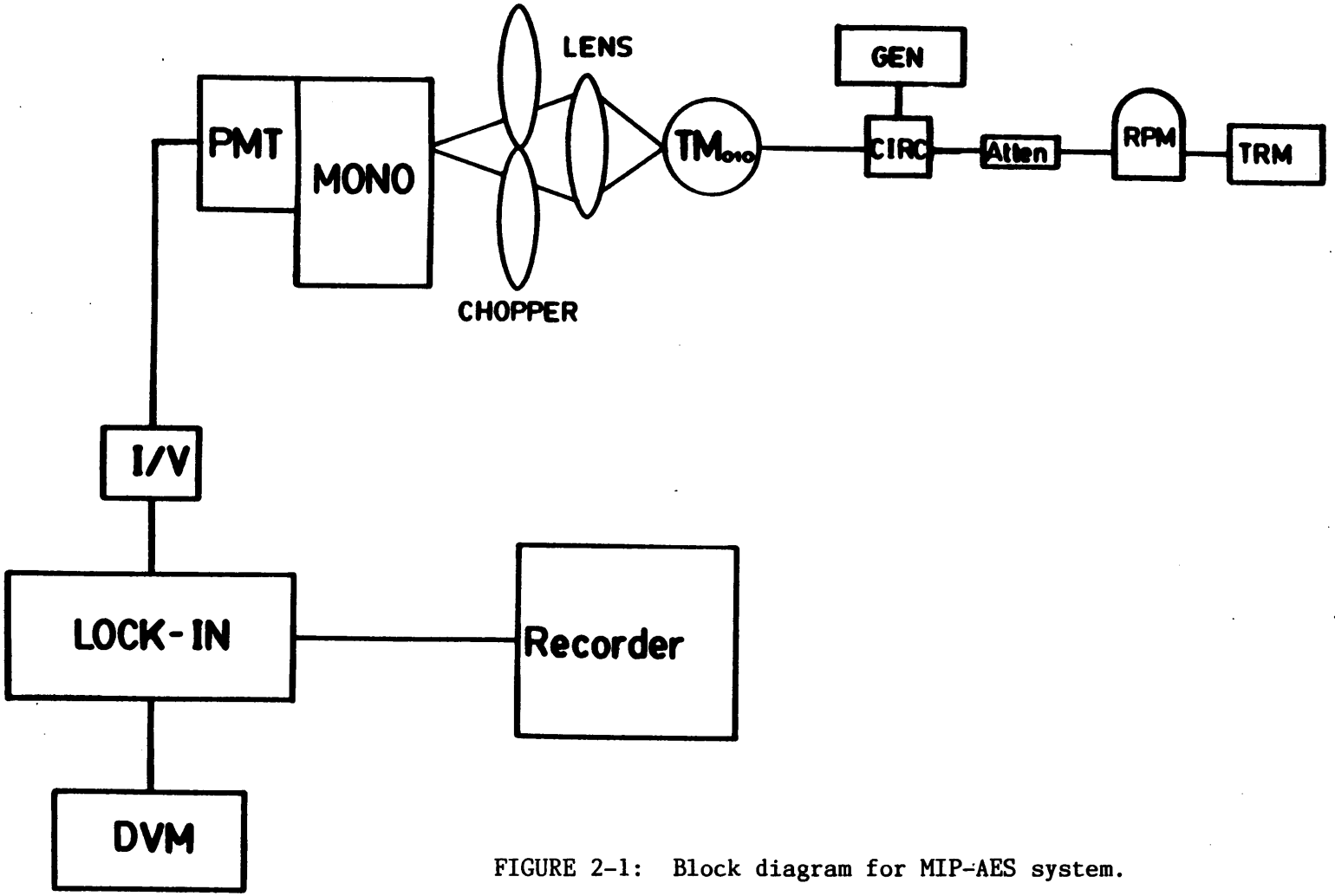

FIGURE 2-1: Block diagram for MIP-AES system.

TABLE 2-1: Equipment used in MIP-AES

Components	Model/Size	Manufacture
Microwave Cavity	H.E.F. cavity	Laboratory built
Generator	120 W	Kiva Instrument Co.
Circulator	Model MA-HC 7238	Microwave Assoc.
Attenuator	Model A8510N	Engleman Microwave
Termination	Model 80M	Bird Electronics
Discharge Tube	Tangential	Laboratory built
Coaxial Cable	RG 214	Times Fiber Comm.
Monochromator	Model EU-700	Heath
I/V	Model A1	Thorton EMI
PMT	Model EU-701-93	Heath
Nebulizer	concentric	J. C. Meinhard
Spray Chamber	Scott	Laboratory built
Chopper	Model 125A	EG & G
Lock-in	Model 5101	EG & G
Lens	f/3, suprasil	Oriel Corp

TABLE 2-2: Operational Parameters for MIP-AES

Foward Power	70 W
Reflected Power	0 W
Observation Height	1-2 mm above cavity
Nebulizer Uptake	0.91 mL/min
Auxiliary Argon Flow	0 mL/min
Total Argon Flow	1 L/min
Probe Penetration	75%

To the cavity was applied 70 W of power from the Kiva generator. A tungsten wire attached to a rubber policeman (for insulation) was inserted into the quartz torch within the TM_{010} cavity. The wire was then inductively heated by the electric and magnetic fields, causing a "seed" of the argon gas to iqnite the plasma. The plasma was then tuned to 0 W reflected power by adjusting a quartz sliding rod and by utilizing the electrical properties of an antenna probe [6].

It should be noted that after several hours of operation, neither cavity nor connectors were observed to heat up, but remained "cool to touch". These observations indicated that the cavity was critically coupled to the generator and no significant power loss were occuring in the cavity, cables, or connectors.

The reflected power was monitored by an external meter (see Figure 2-1). Although the generator provided a built-in means of measuring the incident and reflected power, the instrumental incident power meter revealed the amount of power sent to the generator's magnetron instead of the amount of power sent to the cavity and thus the plasma. This reading is not only misleading to the researcher, but provides the basis for misleading power transfer data.

To obtain an accurate measurement of the power delivered to the cavity and reflected from the generator, a

T circulator, an attenuator, and a termination device was employed (see Table 2-1). In this "T" configuration, power is sent from the generator to the plasma, and the reflected power travels from the generator back to the circulator where it is attenuated by a 10 dB attenuator, displayed on the external meter, and terminated by the termination device.

As a result, the T configuration has proven useful in four ways:

1. No power is reflected back to the generator, thus yielding a longer lifetime for the generator's magnetron.

2. Since the cavity can be accurately tuned to 0 W reflected power, it provides a means of monitoring power levels to achieve a "critical coupling" between the generator and the microwave cavity.

3. It provides a means of calibrating the generator by connecting the attenuator/meter/terminator directly to the generator. The actual power leaving the generator is indicated on the external meter and can be used to calibrate the instrument's incident power meter.

4. It provides an accurate means of reporting applied and reflected power, thus preventing misleading analytical results. This allows researchers to better compare data.

It should be noted that the plasma can be lit while aspirating 1 mL/min water with power levels of 50 W. (On rare occasions when the plasma went out during these studies, it was easily relit with the accumulated water exiting the top of the torch in a spiral "sprinkler" type fashion. The presence of air in the spray chamber did not affect the operation of the plasma. Concentrated methanol could be directly aspirated into the cavity, and propane/Ar mixtures couls be introduced into the plasma without causing stability problems. The organic gases caused a blue tail similar to that of a Bunsen burner.)

Microwave Leakage

Microwave leakage for this system was inspected and was found to be 0.5 mW/cm^2 and is established to be lower than most moderate or high power MIPs [13,20]. We found that this value is less than the allowable leakage for household microwave ovens (1 mW/cm^2 at 5 cm) [21].

Sample Introduction

Aqueous samples were directly aspirated into the plasma using a Meinhard concentric nebulizer and Scott-type spray chamber. No desolvation system was employed. After ignition of the plasma, the auxiliary argon flow was turned off so that the plasma was sustained only by the nebulizer

gas flow (1.0 L/min Ar). Sample uptake rate was approximately 0.9 ml/min. The presence of this amount of water in the plasma gas was not observed to affect the plasma using this highly efficient cavity.

Torch Design

A stable plasma was produced using a torch similar to that employed in ICP systems [22]. The torch consisted of two concentric quartz tubes, an outer one of 8 mm i.d. and the inner one of 0.5 mm i.d.. The inner tube has a length of 3 cm while the length of the outer tube is 5.5 cm. A stable tangential flow is produced by forcing the argon gas to flow around the central tube.

The argon flow introduced tangentially contains the analyte aerosol and sustains the plasma. The center tube is constricted by using a 1 in. length of sealed tyqon tubing. Thus the central tube is only used to produce the tangential flow.

Plasma Features

After ignition, the tangentially formed plasma filled the discharge tube and extends 3-4 cm from the top of the resonance cavity. The resulting plasma (with aqueous sample introduced) contains three distinct regions, denoted by a difference in color. These regions are a result of

electrical breakdown of the plasma gas and consist of a pink zone centered in the discharge tube and a blue glow surrounds it. This blue glow is then surrounded by a green afterglow. The green afterglow forms a sheath around the blue region and apparently results from the excitation of water and oxygen entrainment in the plasma.

When aerosol is not present in the plasma, two regions were present. These two regions are a pink zone and a blue zone which extends outside the discharge tube.

The length and intensity of the above regions depends on flow rate, applied power, and the length of the discharge tube.

Plasma Stability

Operation time of the plasma exceeded 8 hours with a cavity temperature not exceeding 30°C. To date, the torch lifetime has exceeded 2 years with little or no etching.

Reagents

All chemicals used were analytical reagent grade. Water was deionized. Stock solutions of all metals were purchased as 1000 ppm (Buck Scientific, Inc.) or prepared following standard procedures. Volumetric dilution of these solutions were made to obtain the desired concentrations. The plasma

gas used was Airco analytical grade argon.

Excitation Temperature

An iron solution of 1000 ppm was aspirated into the argon plasma and the relative intensity of the iron lines in the spectral region of 360-470 nm were measured. The excitation temperature was as determined from a logarithmic form of the Boltzman equation [23].

$$\ln(I\lambda_{ki}/(g_k A_{ki})) = E_k/(kT_e)$$

where I = relative intensity of specific iron lines

λ_{ki} = wavelength of known iron transitions

g_k = statistical weight of the upper state

A_{ki} = transition probability

E_k = excitation energy of the excited state

k = Boltzman constant

T_e = excitation temperature

A plot of $\ln(I_{\lambda ki}/(g_k A_{ki}))$ vs E_k yields a straight line with a slope equal to $1/kT_e$. Table 2-3 summarizes the transitions, statistical weight, transition probabilities and excitation energies used for the measurements in this study.

TABLE 2-3 : Spectroscopic data for Excitation Temperature measurements using Fe(I) emission lines.

Wavelength (nm)	E_{ki}	g_k	A_{ki}
358.1	34844	13	1.03
360.9	35856	5	0.797
371.9	26875	11	0.163
373.5	33695	5	0.886
381.6	38175	7	0.948
382.0	33096	7	0.638

Limits of Detection

The IUPAC definition (1975) for the limit of detection states that " the limit of detection, expressed as a concentration, cL (or amount, qL), is derived from the smallest measure, xL, that can be detected with resonable certainty for a given procedure" [24]. The definition was further reinstated by the American Chemical Society (1980), which states " the limit of detection is the lowest concentration of an analyte that an analytical process can reliably detect" [25].

The mathematical approach to the IUPAC definition is as follows:

$$cL = ksB/m$$

where cL = limit of detection

k = numerical factor chosen inaccordance with the confidence level

sB = standard deviation

m = analytical sensitivity

According to Long and Winefordner in a recent review on Detection Limits, a value of k equal to 3 should be used to calculate detection limits in spectroscopy. A k of 3 represents a confidence level of 99.86% [26].

The limits of detection were calculated as prescribed by IUPAC guidelines. For each calculation, 20 background readings were taken. The analytical sensitivities were calculated from the working curves of the element, which spanned a range of at least two orders of concentrative magnitude. Although not suggested a value of 2 for k has been used so that these values may be compared to those already in the literature for MIP-AES.

Data Collection

The plasm was translated in the X and/or Y direction via translation stages (NRC) to yield the optimum observation zone. The optimum height was found to be 1-2 mm above the cavity. Signals were processed via a lock-in amplifier and an Apple IIe computer equipped with a 12 bit A/D converter. Data for limits of detection and emission profiles were stored in memory.

Results and Discussion

Power Levels

In order to be able to adequately report the power levels at which this low powered MIP was operated, the forward meter of the microwave was calibrated by directly feeding the output into the attenuator/meter/terminator (as

described in the Experimental section). The generator was capable of producing forward power levels of up to 72 W. With the meters calibrated, it was noted that the plasma could easily be sustained by the Ar flow of the nebulizer alone, thus allowing for the introduction of 0.9 mL/min of sample using only 50-70 W of forward power. Neither the introduction of the sample nor the reduction in the applied power levels resulted in reflected power (0 W), therefore no adjustments in the cavity tuning were necessary. Power levels below 50 W did necessitate tuning adjustments; however, with careful tuning a toroidal plasma was produced using only 36 W of forward power (0 reflected power) while aspirating the sample. This confirms the earlier calculation [18] of the minimum energy required to operate an MIP with direct nebulization and the effiency of the highly efficient cavity.

Excitation Temperature

The temperature of the plasma at 70 W forward power using 1.0 L/min Ar and the aspiration of 0.9 mL/min aqueous solutions was measured using the Fe slope method [27]. At an observation height of 2mm above the cavity, the excitation temperature was measured to be 4500 +/- 90 K.

Profiles

In order to evaluate the cavity as an atom and excitation cell, plots of analyte emission versus observation heights were constructed for a variety of elements. In Figure 2-2, a background subtracted plasma emission profile of Na(I) is shown using a 70W plasma and direct sample introduction. In this profile, the relative intensity is plotted against the viewing height above the radial face of the cavity with the torch flush against the face. The optimum response for emission was observed at a height of 2 mm, while the response was greatly diminished at higher viewing regions of 10-20 mm. This optimum region at 2 mm was noted for other elements studied and was chosen as the viewing height for measurement of working curves and calculation of detection limits.

Working Curves

With this method of direct sample introduction, there existed some concern regarding the effect of high salt samples on the plasma's ability to vaporize and excite the analyte. In Figure 2-3, a background subtracted working curve for Na is shown using the operating conditions outlined in Table 2-2. This log-log plot, which extends from 0.01 ppm to 1000 ppm, is quite linear over five orders of concentrative magnitude and possesses a slope of 0.9998.

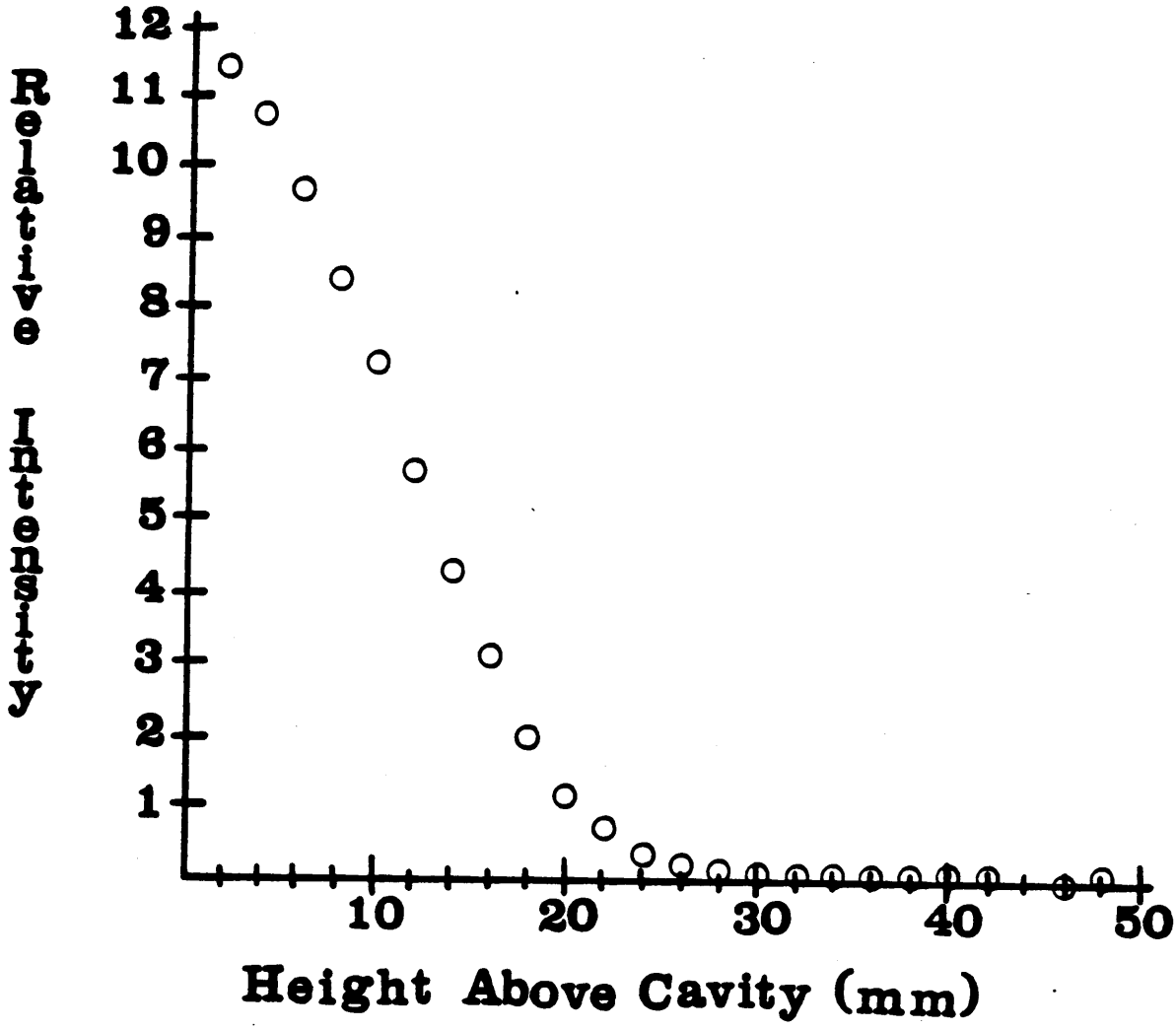

FIGURE 2-2: The emission profile of a 10 ppm Na solution using direct nebulization. Zero millimeter represents flush with the top of the cavity.

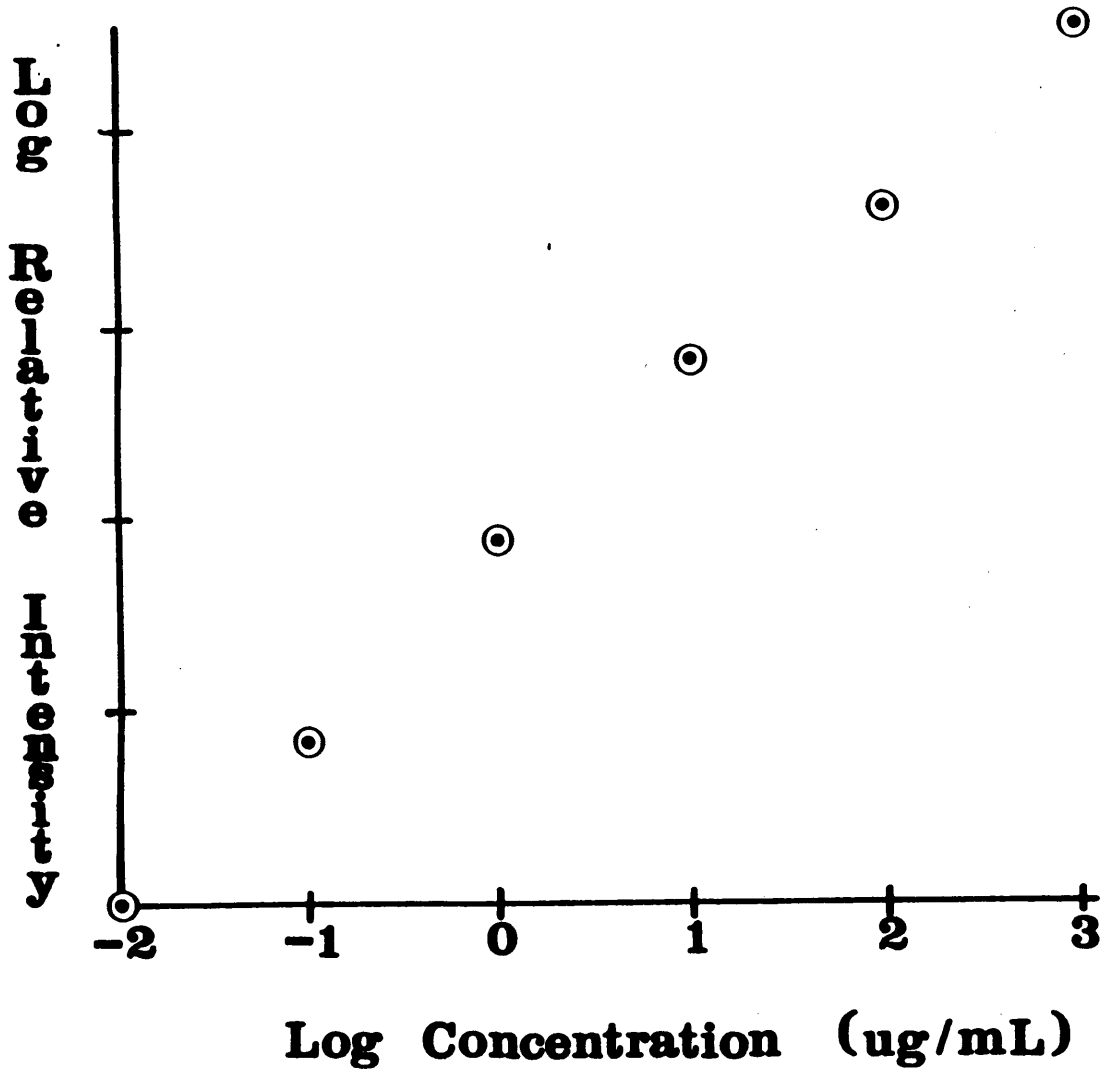

FIGURE 2-3: Na calibration curve using MIP-AES.

At larger Na concentrations, no bending of the working curve is noted, indicating that the plasma is able to vaporize and excite these high analyte concentrations and is free from self reversal.

Limits of Detection

An important parameter in gauging the analytical utility of this direct sample introduction MIP system is the limit of detection for an element. In Table 2-4, a listing of detection limits for this system (column 1) and for other MIP systems are presented. The values were calculated in accordance with IUPAC guidelines. The data in column 2 were obtained by Beenakker et al. using a 150 W plasma with a crossflow nebulizer and optional heated spray chamber. These values, however, were calculated with only 10 background readings and an assumed RSD of 0.004-0.006 [12]. The data in column 3 were obtained by Haas at al. using a higher power MIP (300-500 W) cavity with direct sample introduction [13]. The data in the fourth column were obtained by Ng and Shen using a Beenakker cavity and moderate power (115 W), and MAK nebulizer for direct sample introduction [14]. The limits of detections are described here with a k of 3.

As noted by comparing the data, the system described in this paper (column 1) is generally an order of magnitude

TABLE 2-4: MIP-AES Detection Limits in ppm (k=2).

Element	c_L^1	c_L^2	c_L^3	c_L^4
Ag	0.12	0.006		
Al	1.4	0.4	0.65	
Ba	0.18			
Ca(I)	0.040			
Ca(II)	0.27			
Co	1.8	0.15		
Cr	8.0	0.15	0.004	0.062
Fe	0.65		0.008	
K	0.024			
Li	0.043	0.001		
Mg	0.63	0.005		
Mn	6.9	0.05	0.0039	0.018
Na	0.002			
Sr	0.025	0.01		0.013
Zn	0.042		0.0023	

Note: Two significant figures are used for comparative purposes only.

1 This work.

2 See reference 12.

3 See reference 6.

4 See reference 14.

inferior to the other data. This lack of sensitivity may result from the fact that (1) the generator used in this study had a limitation of 72 W forward power and/or (2) a 0.34 m monochromator with a resolution of 2 A was employed. In other studies, a 0.5 m or greater monochromator was used. Applied powers of 100-150 W produce a greater energy density in the plasma and led to enhanced analyte signals. A monochromator with finer resolution decreases the stray light registered in the detection system, thus enhancing the sensitivity.

As regards comparison to the data in the fourth column, Ng and Shen used, in addition to the 0.5 m instrument, a MAK nebulizer for sample introduction into the 115 W plasma. In terms of droplet distributions, the MAK produces a much smaller sized droplet than the Meinhard used in this work [28]. Because droplet size affects the desolvation and vaporization times of the analyte as well as the solvent loading, smaller droplet sizes should result in decreased detection limits. In particular, the detection limits are 2 orders of magnitude superior for Cr and Mg using the MAK nebulizer. However, the detection limit for Sr is not statistically different. Since these metals have higher dissociation energies for their oxides, the decrease in sensitivity for Cr and Mg in this work may be the result of spectral noise rather than insufficient plasma power, as

compared to Ng and Shen's work.

Interferences

The analytical utility of this direct sample introduction MIP as an atom and excitation cell for atomic spectrometry was estimated by examining several interferences that occur in flames and plasmas. For the ionization interference, the effect of Na on Ca signals was studied; for vaporization interference, the effect of PO_4^{3-} on Ca signals was studied.

Ionization

The effect of an easy ionizable element, Na, on Ca(I) background subtracted emission signals is shown in Figure 2-4. Using the operational parameters outlined in Table 2-2 and a 10 ppm Ca solution, the effect of Na concentrations from 0.01 ppm to 1000 ppm were observed. At low Na levels, 0.01-1.0 ppm, no discernible effect of the easily ionizable element, EIE, on Ca(I) is seen. At levels of 10-100 ppm Na, a maximum 10% increase in Ca(I) was recorded with the presence of the EIE. However, at 1000 ppm Na, the Ca(I) signal increased by 300% with this level of EIE present in the plasma. This large increase indicates that there is significant Ca ionization occuring in the plasma; at these low plasma powers, matrix matching of standards and samples

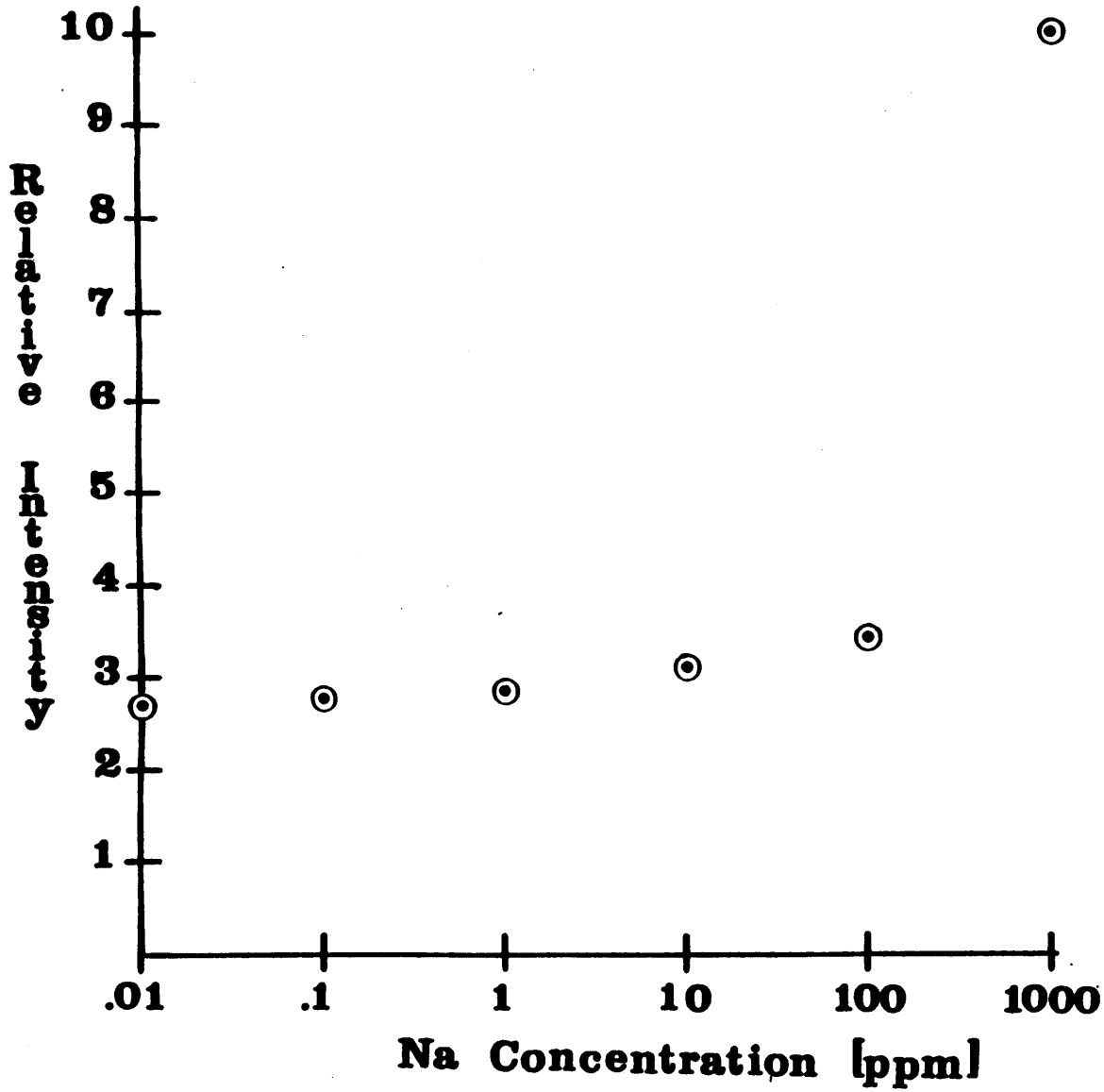

FIGURE 2-4: The effect of Na on the emission signal of a 10 ppm Calcium solution.

must be considered using this plasma source as an analytical tool.

Vaporization Interference

To evaluate the ability of this plasma to vaporize refractory compounds, the classic Ca^{2+}/PO_4^{3-} vaporization experiment was conducted using the operating conditions outlined in Table 2-2 and a 10 ppm Ca solution. The results of this experiment were background subtracted and are plotted in Figure 2-5. As seen in this plot, the Ca(I) signal falls by 30% with the addition of PO_4^{3-} to achieve a PO_4^{3-}/Ca^{2+} ratio of 1:1. This level of depression remains essentially unchanged through a PO_4^{3-}/Ca^{2+} ratio of 100:1. At a level of 1000:1, however, the Ca(I) signal drops by 80%.

This behavior is fairly consistent with other data observed for MIP systems. At a PO_4^{3-}/Ca^{2+} ratio of less than 1:1, the condensed phase compound is formed. The addition of more PO_4^{3-} does not affect the Ca(I) signal except at extremely high PO_4^{3-} concentrations. It should be noted that the PO_4^{3-} depression caused only a 30% reduction in the Ca(I) signal as compared to a 70% depression which occurred with an earlier MIP system. Although the PO_4^{3-}/Ca^{2+} depression is very sensitive to droplet size formation and

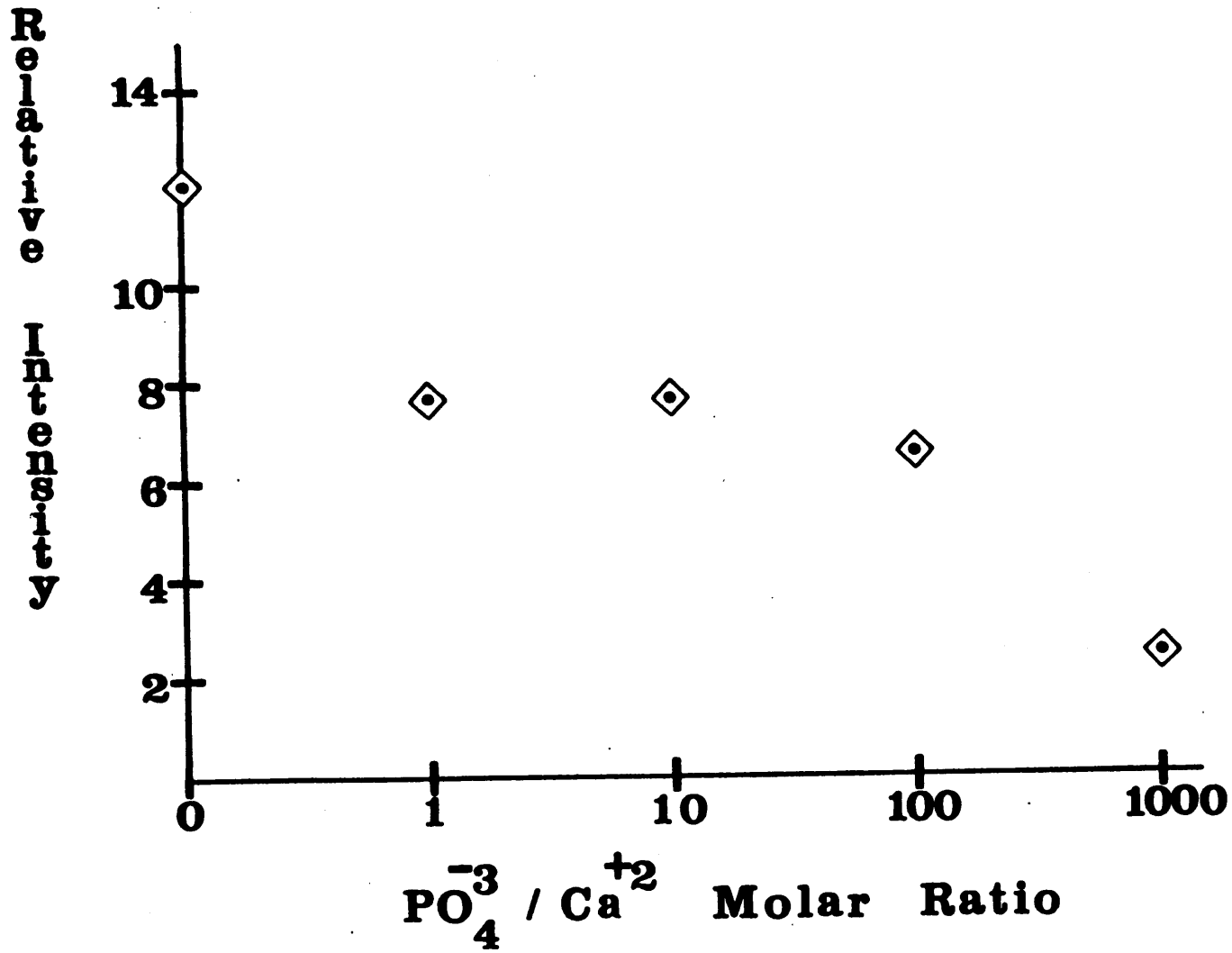

FIGURE 2-5: The effect of PO_4^{3-} an Ca^{2+} atomic emission signal. Calcium concentration = 10 ppm.

distribution [29] is indicative of the power of the MIP to promote analyte vaporization and dissociation. This system, using direct sample introduction into the MIP, is prone to vaporization interferences, but less so than other MIPs.

CONCLUSION

With the use of the highly efficient TM_{010} cavity, the direct introduction of aqueous samples into a low power MIP with no desolvation system has been achieved. The combination of nebulizer/torch and cavity permits a toroidal plasma sustained by the Ar output of the nebulizer alone. Although the limits of detection using this system in the emission mode are a factor of ten higher than those of previous MIP-AES studies, the fact that extremely low powers and a medium resolution monochromator were employed to obtain these values may explain these inferior values. In terms of ionization and vaporization interferences, the results show this system compares favorably with those of other MIP-AES systems.

CHAPTER 3

ATOMIC FLUORESENCE SPECTROMETRY

The lack of interest in direct nebulization of aqueous samples imto the microwave induced plasma is due to the well known fact that the MIP has a low kinetic temperature and low energy density which does not allow for sufficient desolvation and excitation of liquid samples.

A possible solution of using a low wattage plasma for spectrochemical analysis for direct aqueous nebulization is presented in this chapter. This solution lies in the application of atomic fluoresence spectrometry, AFS. In the AFS mode the MIP need only to dissociate the analyte into atomic vapor phase atoms, for excitation is accomplished by source radiation rather than by thermal means. In this study Xe-Arc lamp and hollow cathode lamps will be used as excitation sources.

In the AFS approach using hollow cathode lamps, the primary wavelength discrimination is not performed by the high resolution monochromator, but instead is performed by the monochromatic source. Similar systems have been very successful using the inductively coupled plasma [30].

The application and evaluation of AFS to the MIP is the topic of this chapter. Covered in this chapter includes detection limits using Xe-arc-MIP-AFS and HCL-MIP-AFS, as well as studies of interelemet effects such as ionization

and vaporization interferences.

Reagents

All chemicals used were analytical reagent grade. Water was deionized. Stock solutions of all metals were purchased as 1000 ppm (Buck Scientific, Inc.) or prepared following standard procedures. Volumetric dilution of these solutions were made to obtain the desired concentrations. The plasma gas used was Airco analytical grade argon.

Experimental

The block diagram for our AFS-MIP system is shown in Figure 3-1. Equipment used is listed in Table 3-1 along with their respective manufacture and model number.

In order to provide accurate power transfer data a means of measuring the precise amount of reflected power was used and is termed the "T" configuration. In this T configuration, power is delivered from the generator to the cavity via a 50 ohm RG 214 cable, any refelected power (from the cavity), travels to a circulator, exits and is attenuated and displayed on an external meter, then terminated by a termination device (not illustrated in Figure 3-1.

Aqueous samples were directly aspirated into the plasma using a Meinhard concentric nebulizer and Scott-type spray

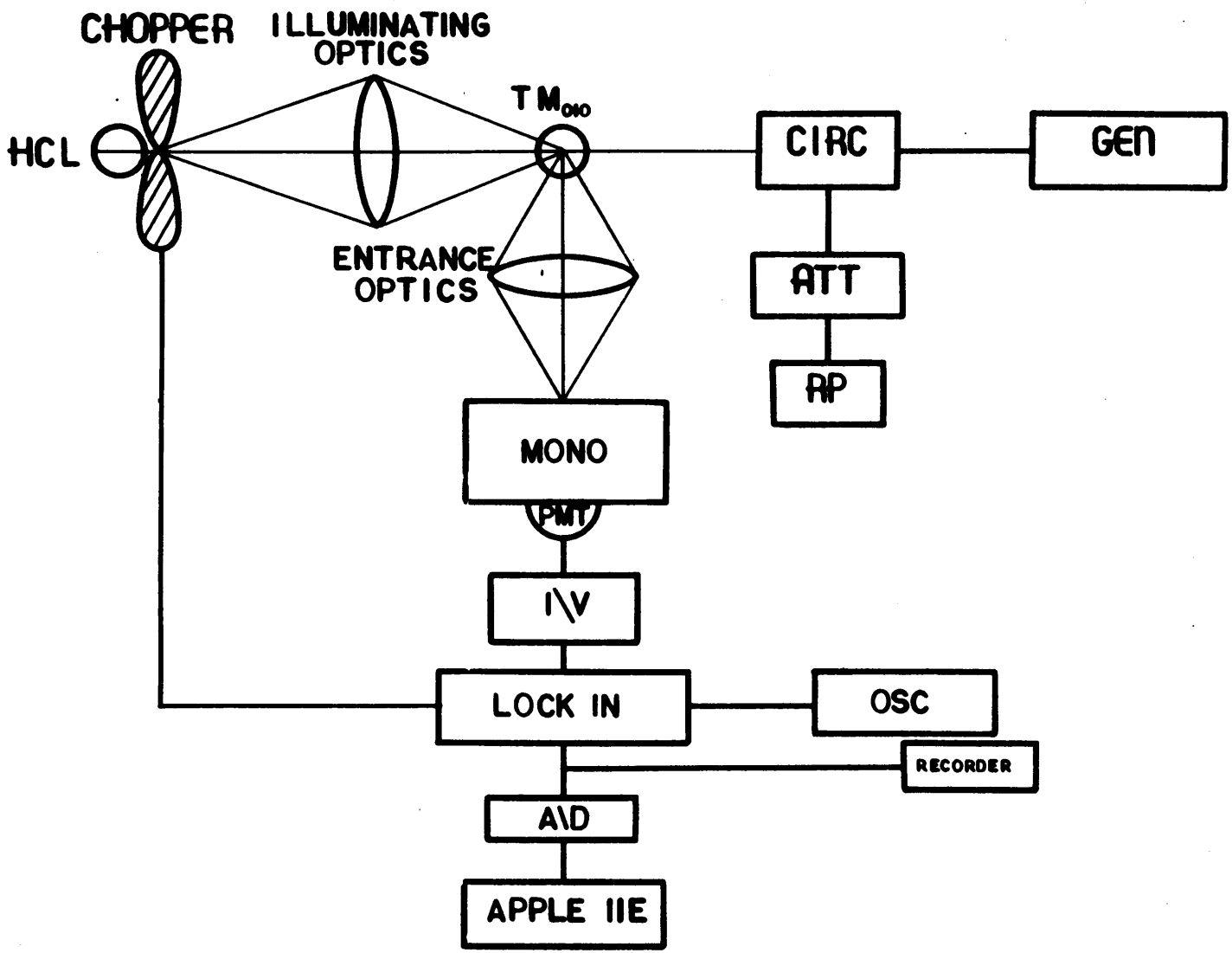

FIGURE 3-1: Block diagram for MIP-AFS system.

TABLE 3-1: Equipment used in MIP-AFS

Components	Model/Size	Manufacture
Microwave Cavity	H.E.F. cavity	Laboratory built
Generator	120 W	Kiva Instrument Co.
Circulator	Model MA-HC 7238	Microwave Assoc.
Attenuator	Model A8510N	Engleman Microwave
Termination	Model 80M	Bird Electronics
Discharge Tube	Tangential	Laboratory built
Coaxial Cable	RG 214	Times Fiber Comm.
Monochromator	Model EU-700	Heath
I/V	Model A1	Thorton EMI
PMT	Model EU-701-93	Heath
Nebulizer	concentric	J. C. Meinhard
Spray Chamber	Scott	Laboratory built
Chopper	Model 125A	EG & G
Lock-in	Model 5101	EG & G
Lens	f/3, suprasil	Oriel Corp
Xe-Arc Lamp	LPS200	PTI
Computer	Apple IIe	Apple Co.

chamber. No desolvation system was employed. After ignition of the plasma, the auxiliary argon flow was turned off so that the plasma was sustained only by the nebulizer gas flow (1.0 L/min Ar). Sample uptake rate was approximately 0.9 mL/min.

Operational Conditions

The operational conditions for MIP-AFS with Xe-Arc lamp and HCL excited AFS are shown in Table 3-2. The chopper was operated at a frequency of 169 Hz. The operational power of the excitation sources were varied to yield the optimum fluoresence intensity.

Data Collection

The plasma was translated in the X and/or Y direction via translation stages (NRC) to yield the optimum observation zone. The optimum height was found to be 4-5 mm above the cavity. Signals were processed via a lock-in amplifier and an Apple IIe computer equipped with a 12 bit A/D converter (Interactive Microware). Data for limits of detection and fluoresence profiles were stored in memory.

Data Presentation

The data presented here are shown as background corrected values. For AFS profiles, the background for each

TABLE 3-2: Operational Parameters for MIP-AFS

Foward Power	60-72 W
Reflected Power	0 W
Observation Height	4-5 mm above cavity
Nebulizer Uptake	0.91 mL/min
Auxiliary Argon Flow	0 mL/min
Total Argon Flow	1 L/min
Probe Penetration	75%
HCL power	15-25 mA
Xe-arc Power	140-150 W

height was computer substracted from the analyte signals. Working curve and interelement plots were similiary treated.

Results and Discussion

In this section, the use of hollow cathode lamps and Xe-arc lamps are explored as an excitation source for atomic fluorescence using a low powered microwave induced plasma. This study consists of examining AFS profiles, working curves, limits of detection, and interelement effects.

Profiles

The knowledge of the position of maximum analyte signal in the plasma tail is important in optimizing the plasma as an atom cell. Figure 3-2 represents the atomic fluoresence profile of a 10 ppm Zn solution using HCL excited MIP at a plasma foward power of 70 W. In this profile the relative fluoresence intensity of Zn is plotted versus the observation height above the face of the cavity.

The maximum intensity was observed at a height of 4 mm above the top of the cavity, then diminishes higher in the plasma tail (i.e. 10-20 mm).

It should be noted that at 2 mm above the top of the cavity there existed a small decrease in the fluoresence intensity. This decrease in intensity could be attributed

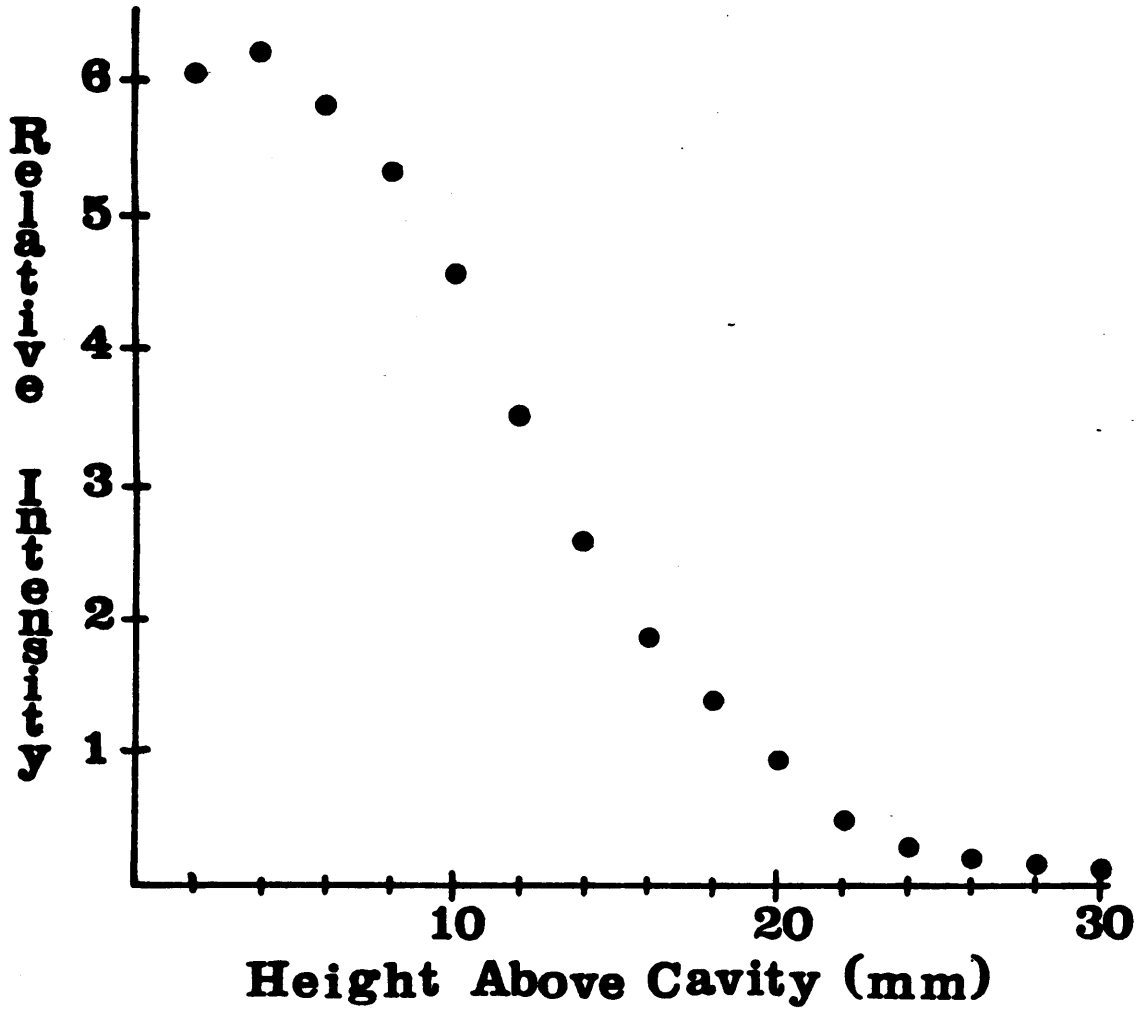

FIGURE 3-2: The fluoresence profile of a 10 ppm Zn solution. Zero millimeter represents flush with the top of the cavity.

to an increase in plasma flicker closer to the plasma "ball". As the observation height is increased closer to the plasma "tail" the intensity increases, in this region of the plasma there exists a decrease in plasma flicker and /or spectral backgroung as well as observations in a cooler region of the plasma. Moreover, the analyte species, at this point has a longer residence time in the plasma, having passed completely through the discharge into the plasma tail. The longer time span permits more complete molecular dissociation of the original analyte species. This behavior was also noted using the Xe-arc lamp.

Working Curves

In Figure 3-3, a HCL-AFS-MIP working curve is presented for Zn using the operational parameters outlined in Table 3-1. The concentration of this log-log plot extends from 0.01 ppm to 1000 ppm and is linear up to over five orders of concentrative magnitude. The slope of this working curve is 0.99998.

Using the HCL-AFS-MIP system there seems to be no bending of the working curve at high concentrations due to self absorption. Although not presented this type of working curve (linearity of at least five orders of concentrative magnitude) was indicitive of other elements studied using both Xe-arc lamp and hollow cathode lamp excited AFS with

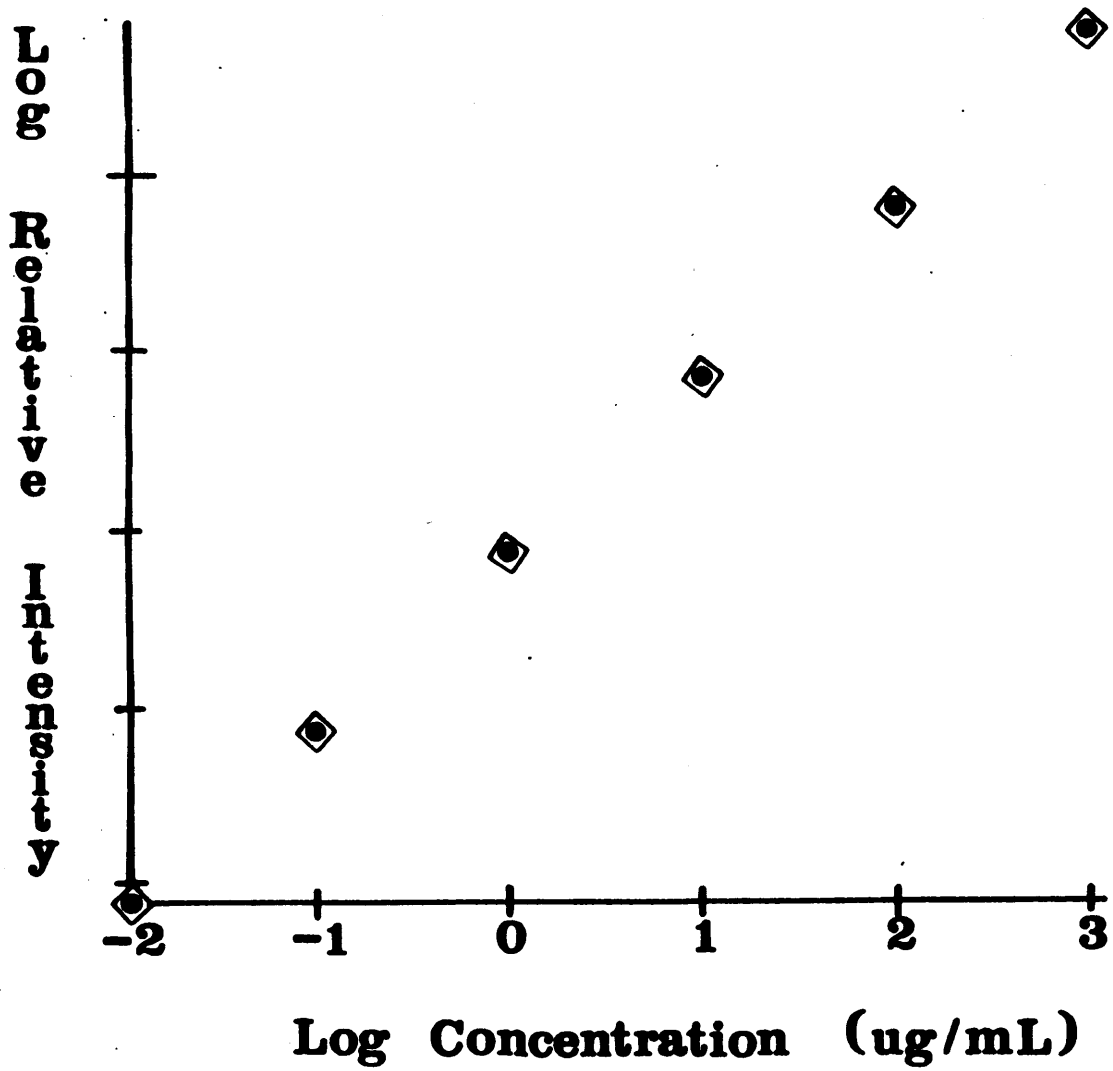

FIGURE 3-3: Zn calibration curve using MIP-AFS.

this low powered MIP.

Limits of Detection

Table 3-3 lists the detection limits for this MIP-AFS system using Xe-arc lamp and hollow cathode excitation. These detection limits are compared to the work of Demers, Busch, and Allemand using pulsed hollow cathode lamp excitation with the ICP [30].

Generally the MIP-AFS detection limits using this system are a factor of 10 worse than those found for ICP-AFS. This increase in detection can be attributed to the use of pulsed hollow cathode lamps with the ICP. The method of pulsed hollow cathode lamp excitation provides a means to produce greater sensitivities and lower detection limits, since the output of the pulsed hollow cathode lamp is typically 100 times brighter than that of non-pulsed hollow cathode lamps. According to Demers, the use of pulsed hollow cathode lamps decreases detection limits in atomic fluoresence spectrometry in the ICP by a factor of 50 [31]. This suggests with the employment of pulsed hollow cathode lamps in this system, detection limits would be on the same order as those in ICP-AFS.

It is interesting to note that for the elements studied that there is not a statistical between Xe-arc-MIP-AFS and HCL-MIP-AFS detection limits using this low powered plasma

TABLE 3-3: MIP-AFS Detection Limits in ppb (k=2).

Element	HCL-MIP-AFS	HCL-ICP-AFS	Xe-arc-MIP-AFS
Ag	40	2	70
Al	700	20	1000
Ba	20	50	40
Li	20	0.4	50
Ca(I)	20	0.4	20
Co	1000	3	1000
Cr	2000	8	2000
Fe	600	10	1000
K	20	0.8	50
Mg	20	0.5	70
Mn	500	3	400
Na	10	0.3	50
Sr	20	2	80
Zn	40	0.4	40

except for the IA and IIA elements.

Ionization Intereferences

The presence of easily ionizable elements, EIE, on atomic signals in plasma emission spectrometry has been well studied. This effect is the result of the easily liberated electrons from the EIE elements affecting the equilibrium balance of the analyte atoms and ions. Generally, as the temperature of the plasma increases, analyte ionization occurs to a greater extent and the the EIE effect is noted. This type of interference has been noted in ICP-AFS where lower applied powers are used [32].

The effect of an EIE on the Ca(I) atomic fluoresence signal is shown in Figure 3-4. At a interferent, Na, concentration of 0.01-1 ppm there exists no discernable effect of the EIE to create an ionization effect. As the interferent concentration increases to 10 ppm the fluoresence intensity of Ca(I) increases by a factor of 50%. The fluoresence intensity continues to increase as the interferent concentration reaches 1000 ppm where a rise of 100 % is noticed.

Since the MIP is not in local thermodymanic equilibrium this type of interference should be expected, therefore the addition of electrons provided by the EIE may play a very important role in the plasma maintance. The sensitivity of

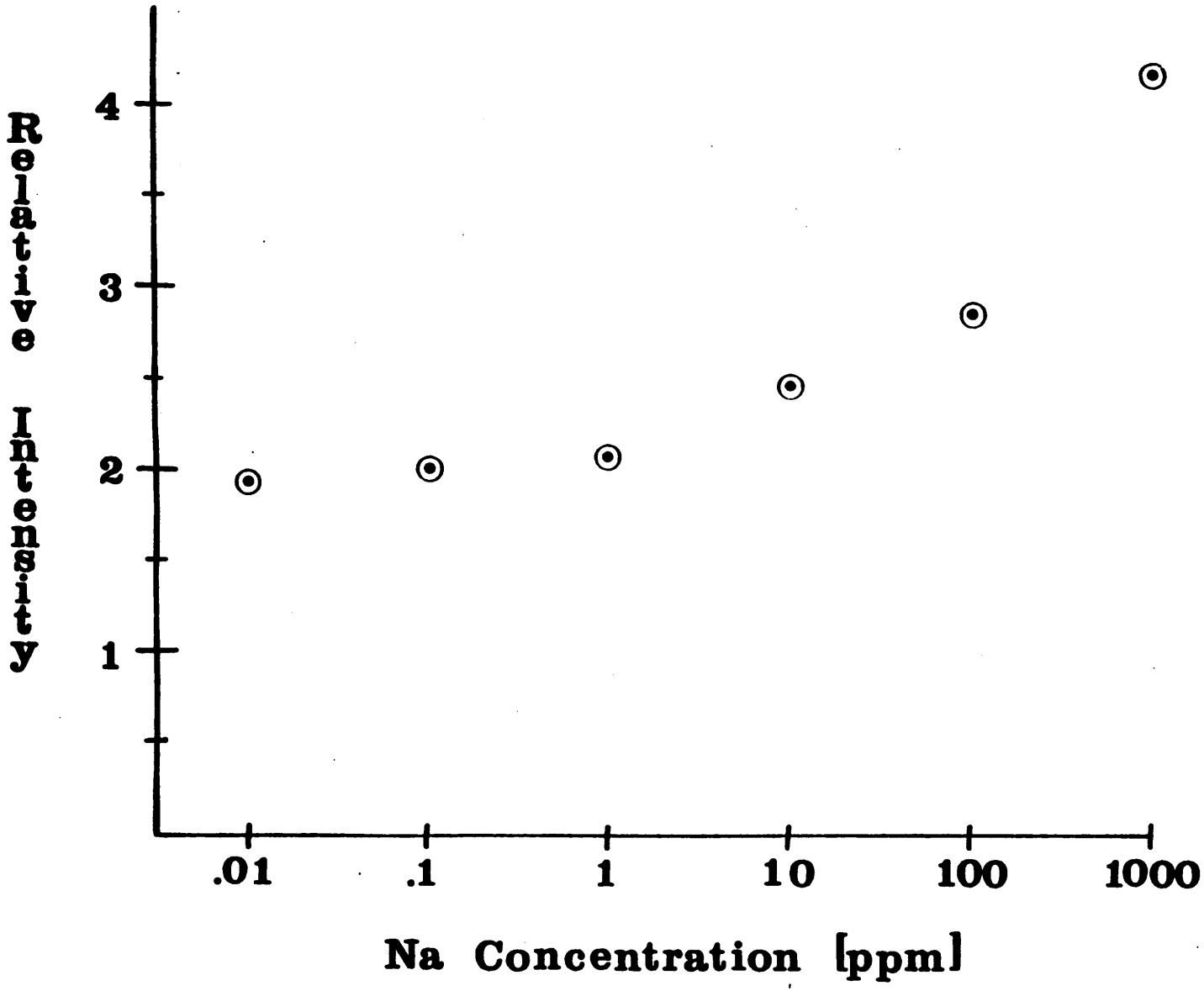

FIGURE 3-4: The effect of Na on the fluoresence signal of a 10 ppm Ca solution.

the fluoresence intensity seems to be very susceptible to the addition and disappearance of electrons in the low power plasma used in this study for Xe-Arc lamp and hollow cathode lamp excited atomic fluoresence.

Vaporization Interferences

Another classic interference that is used to test the effectiveness of an atom cell is the depression of Ca signals by the addition of phospate ions to the analyte matrix. Upon this addition, a refractory $Ca_3(PO)_4$ compound is formed. If the plasma is sufficiently energetic, the refractory compound can be vaporized and dissociated into free atoms, resulting in no reduction of the atomic signal. Figure 3-5 shows the influence of the phosphate on a 10 ppm Ca(I) signal at 422.7 nm using HCL-AFS-MIP and the operational parameters outlined in Table 3-1.

In this plot the classical and important intereference would be expected to occur at 1:0.5 PO_4^{3-}/Ca^{2+} molar ratio. At the of 1:1 PO_4^{3-}/Ca^{2+} molar ratio a depression of 43% occurs. The depression continues to increase where at a 1000:1 molar ratio we find that the orgional intensity has decreased by approximately 65%.

The above results suggests the following: (1) the 70 W MIP is not able to vaporize very refractory compounds (i.e. Ca/PO_X species), (2) a higher power plasma is needed,

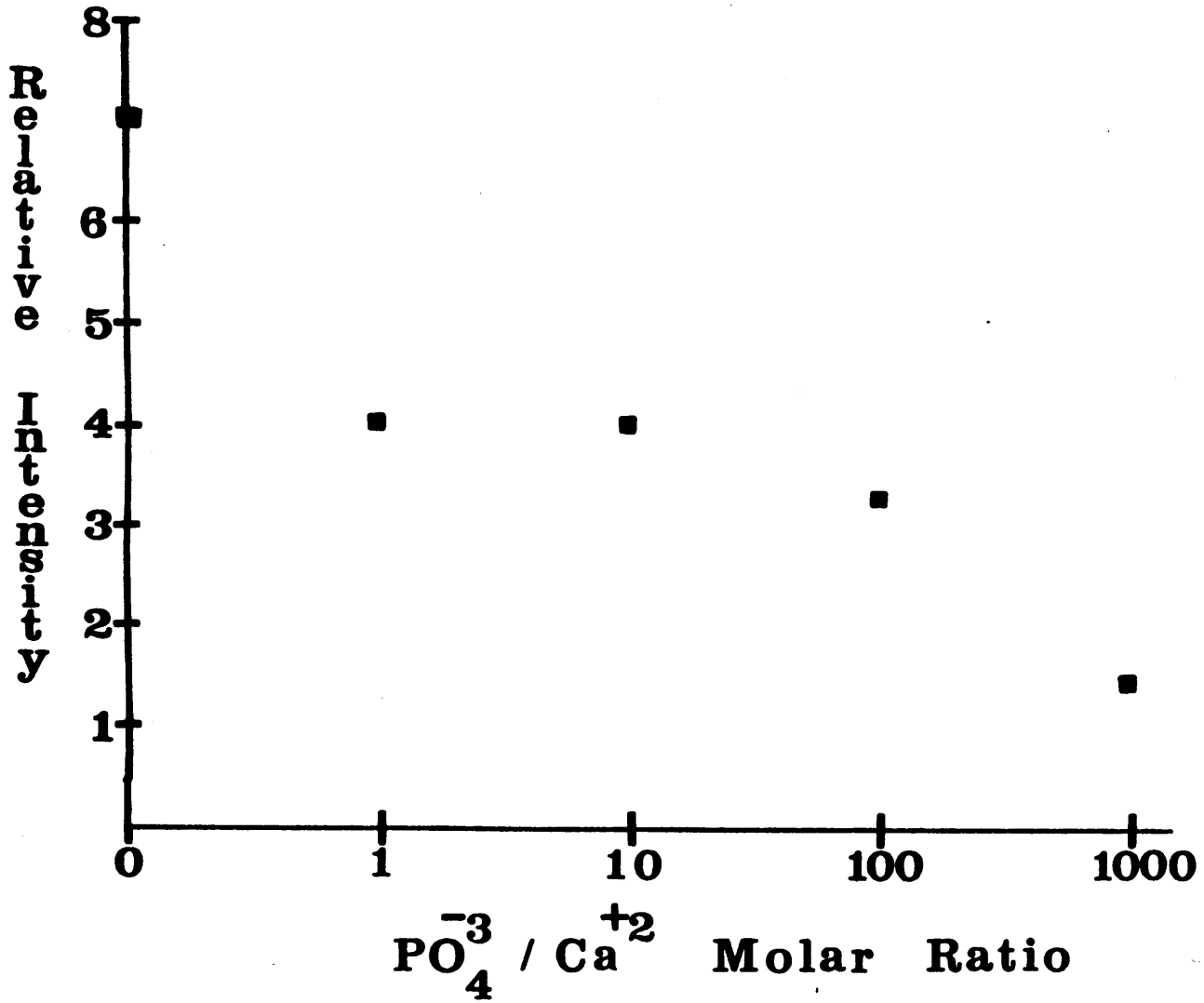

FIGURE 3-5: The effect of PO_4^{3-} on Ca^{2+} atomic fluoresence signal.

and/or (3) the droplet size distribution of the nebulizer does not adequately surfice for this type of experiment.

Similar occurances of the PO_4^{3-}/Ca^{2+} interference have been noticed in ICP-AFS using low wattages [32]. Demers and Allemand showed that this interference can be decreased with an increase in applied power. Due to the limitation of our generator by 72 W, studies of this type were not conducted.

Scatter Interferences

With this method of direct nebulization using a low power plasma, there existed concern regarding intereferences due to scatter of non-vaporized particles in the plasma. This interference was investigated by aspirating a 1000 ppm Al into the plasma while monitoring the fluoresence intensity of Ca and Zn. Using this low power MIP there existed no discernable scatter interference using both excitation sources (Xe-Arc lamp and hollow cathode lamp).

CONCLUSION

This work shows that the MIP has promise as an atom cell for atomic fluoresence spectrometry. It exhibits a large dymanic range over several orders of concentrative magnitude and is relative free from background

interferences. Furthermore, the MIP as an atom cell is virtually free from scattered particulate light even at large concentrations of very refractory elements. Although, matrix matching will be needed due to ionization interferences this MIP is less prone to this type of interference than those employed currently in atomic emission.

The MIP-AFS system described allows for single and multielement determinations. This author feels that the MIP-AFS system has the possibility of becoming a low cost spectrometric technique for routine analysis as well as non-routine analysis.

FUTURE WORK

Further optimization of the MIP-AFS system is needed. It is my feeling that if pulsed hollow cathode lamps or a laser is employment as the excitation source this system would provide detection limits at or near those of the current commercial ICP-AFS system. On the basis of cost, size, and simplicity this type of system is very much needed in the scientific community.

Chromatographic studies should be conducted. This system could prove to be a very reliable elemental selective detector for GC and HPLC. Another chromatographic method, SFC, could be used as a sample introduction device to study the atomization processes in the microwave induced plasma.

REFERENCES

1. A. T. Zander and G. M. Hieftje, Appl. Spectrosc., 35, 375(1981).

2. R. S. Alger, Electron Paramagnetic Resonance: Technique and Applications (New York: Interscience 1968.

3. C. W. Schramm, T. G. Wilson, and J.P. Kinger, Bell System Tech. Journal, 25, 408(1946).

4. C. I. M. Beenakker, Spectrochem. Acta, 31B, 483(1976).

5. J. P. J. van Delan, P. A. de Lezanne Coulander, and L. de Galan, Spectrochem. Acta, 33B, 545(1978).

6. L. G. Matus, C. B. Boss, and A. N. Riddle, Rev. Sci. Instrum., 54, 1667(1983).

7. J. Carnahan, Am. Lab., 31, March 1983.

8. R. K. Skogerboe and G. N. Coleman, Anal. Chem., 48, 611A(1976).

9. J. P. Matousek, B. J. Orr, and M. Selby, Prog. Analyt. Atom Spectrosc., 7, 275(1984).

10. T. H. Risby and Y. Talmi, CRC Crit. Rev. Anal. Chem., 14, 231(1982).

11. R. F. Browner and A. W. Boorn, Anal. Chem., 56, 875A(1984).

12. C. I. M. Beenakker, B. Bosman, F. W. J. M. Bowmans, Spectrochim. Acta, 33B, 373(1978).

13. D. L. Hass and J. A. Caruso, Anal. Chem. 47, 194(1984).

14. K. C. Ng and W. L. Shen, Anal. Chem., 58, 2084(1986).

15. H. Kawaguchi, I. Atsuya, and B. L. Vallee, Anal. Chem., 49, 266(1977).

16. O. Rose, D. N. Muncey, A. M. Yacynych, W. R. Heineman, and J. A. Caruso, Analyst, 101, 753(1976).

17. L. R. Layman and G. M. Hieftje, Anal. Chem. 47, 194(1975).

18. G. M. Hieftje, Department of Chemistry, Indiana University, personal communication.

19. B. Burns and C. B. Boss, North Carolina State University, unpublished work.

20. D. L. Hass, J. W. Carahan, and J. A. Caruso, Appl. Spectrosc., 37, 82(1983).

21. Tom Smithwick, Department of Safety, Virginia Tech.

22. R. Deutch, Indiana State University, Ph.D. dissertation.

23. R. H. Tourin, Spectroscopic Gas Temperature Measurements, Elsevier, New York, 1962, p. 47.

24. "Nomenclature, Symbols, Units, and their Usuage in Spectrochemical analysis II," Spectrochim. Acta, 33B, 242(1978).

25. "Guidlines for Data Acquisition and Data Quality Evaluation in Enviromental Chemistry," Anal. Chem., 52, 2242(1978).

26. G. L. Long and J. D. Winefordner, Anal. Chem., 55, 713A(1983).

27. D. J. Kalnicky, V. M. Fassel, and R. N. Kinsey, Appl. Spectrosc., 31, 137(1977).

28. R. F. Browner, Department of Chemistry, Georgia Tech, personal communication.

29. G. L. Long and C. B. Boss, Anal. Chem., 54, 624(1982).

30. D. R. Demers, D. A. Bush, and C. D. Allemand, Am. Lab., March 1982, p. 167.

31. D. R. Demers, Baird Corporation, personal communication.

32. D. R. Demers and C. D. Allemand, Anal. Chem., 53, 1915(1981).

The vita has been removed from the scanned document